An externally modulated, noise-driven switch for the regulation of SPI1 in Salmonella enterica serovar Typhimurium

Bailly-Bechet, Marc ; Benecke, Arndt ; Hardt, Wolf Dietrich ; Lanza, Valentina ; Sturm, Alexander ; Zecchina, Riccardo

Abstract: In this work we consider the regulation system present on the SPI1 pathogenicity island of Salmonella enterica serovar Typhimurium. It is well-known that HilA is the central regulator in the overall scheme of SPI1 regulation and directly binds to virulence operons and activates their expression. The regulation of the expression of HilA is via a complex feed-forward loop involving three transcriptional activators: HilC, HilD and RtsA, and the negative regulator HilE. Our aim is to model this regulation network and study its dynamical behavior. We show that this regulatory system can display a bistable behavior relevant to the biology of Salmonella, and that noise can be a driving force in this system.

DOI: https://doi.org/10.1007/s00285-010-0385-1

Noname manuscript No.
(will be inserted by the editor)

An externally modulated, noise-driven switch for the regulation of SPI1 in *Salmonella enterica* serovar Typhimurium

Marc Bailly-Bechet · Arndt Benecke · Wolf Dietrich Hardt · Valentina Lanza · Alexander Sturm · Riccardo Zecchina

the date of receipt and acceptance should be inserted later

M. Bailly-Bechet
Université Lyon 1; CNRS UMR 5558, Laboratoire de Biométrie et Biologie Evolutive
F-69622, Villeurbanne, France
Tel: +33-4-72432909
Fax: +33-4-72431388
E-mail: marc.bailly-bechet@univ-lyon1.fr

A. Benecke
Institut des Hautes Études Scientifiques — CNRS USR3078
F-91440 Bures-sur-Yvette, France
Tel.: +33-1-60926665
Fax: +33-1-60926609
E-mail: arndt@ihes.fr

W.-D. Hardt
Inst. of Microbiology, ETH Zürich
CH-8093 Zürich, Switzerland
Tel.: +41-44-632-5143
Fax: +41-44-632-1129
E-mail: hardt@micro.biol.eth

V. Lanza
Department of Physics, Politecnico di Torino
10129 Torino, Italy
Tel.: +39-011-0907387
Fax: +39-011-0907399
E-mail: valentina.lanza@polito.it

A. Sturm
Inst. of Microbiology, ETH Zürich
CH-8093 Zürich, Switzerland
Tel.: +41-44-632-3357
E-mail: sturm@micro.biol.ethz.ch

R. Zecchina
Department of Physics, Politecnico di Torino
10129 Torino, Italy
Tel.: +39-011-0907323
Fax: +39-011-0907399
E-mail: riccardo.zecchina@polito.it

Abstract In this work we consider the regulation system present on the SPI1 pathogenicity island of *Salmonella enterica* serovar Typhimurium. It is well-known that HilA is the central regulator in the overall scheme of SPI1 regulation and directly binds to virulence operons and activates their expression. The regulation of the expression of HilA is via a complex feed-forward loop involving three transcriptional activators: HilC, HilD and RtsA, and the negative regulator HilE. Our aim is to model this regulation network and study its dynamical behavior. We show that this regulatory system can display a bistable behavior relevant to the biology of *Salmonella*, and that noise can be a driving force in this system.

Keywords *Salmonella* · pathogenicity · regulatory network · bistability · noise

1 Introduction

Among bacteria, *Salmonella* serovars are responsible for numerous infections and diseases, ranging from mild gastroenteritis to life-threatening typhoid fever. Infections propagate through contaminated water and food, and the typhoid fever kills more than 600 000 people each year (WHO, 1997). After ingestion, *Salmonella* colonizes the small intestine and is able to internalize into epithelial cells, its first target in the mammalian body. This internalization phase requires the injection of effector proteins into the host cell cytoplasm, which is mediated by a type III secretion system genetically encoded on the so-called *Salmonella* pathogenicity island 1 (SPI1) [11]. Type III secretion systems are needle-like structures which are widespread among bacteria; *Salmonella* contains two of them – encoded within SPI1 and SPI2 –, which are sequentially activated during infection, one for internalization in epithelial cells and the second for survival and growth within macrophages [5].

Control of the expression of the SPI1 genetic island is a crucial process during the progress of the infection. The main transcriptional regulator, HilA, encoded itself on SPI1, has been shown to be able to induce the invasion by inducing expression of the *inv/spa* operon [3]. HilA expression itself is regulated by a complex network of activation and repressions, which is able to integrate and filter signals from the environment to activate the internalization process in the correct niche, i. e. the host's intestine [2,21]. Interestingly, SPI1 expression was found to be bi-stable, yielding "on" and "off" subpopulations under inducing environmental conditions [1,20,25,28] and cooperation between both sub-populations has been proposed to enhance the pathogen's survival in the infected host [1]. The "on" subpopulation is thought to trigger diarrheal disease, while the "off" subpopulation benefits from the altered environment of the inflamed gut and propagates the genotype. Thus, it was of interest to gain a deeper understanding of the mechanisms regulating SPI1 expression. The central core in this regulatory network is a triangular structure formed by RtsA, HilD and HilC [10] (Fig 1, bold, black arrows). The regulations among these genes and their role in pathogenesis are under intense experimental scrutiny (see e.g. [28]). HilD, HilC and RtsA are thought to form a triangular network system of regulators positively regulating each other, while HilE can regulate this system by acting as a negative regulator of HilD (Fig. 1, $\perp$ arrow). In turn, HilD, HilC and RtsA are positive regulators of HilA, the master regulator of SPI1 expression (Fig. 1, grey). Two recent reports have developed models for different parts of this gene regulation network [14,28]. Ganesh et al. have developed mathematical models to explain the effect of the regulator SirA on the average

activity of the HilD-HilC-RtsA-HilA signalling network, without focusing on stochastic differences between different individual or subpopulations. In contrast, Temme et al. have studied at the single cell level the induction and relaxation dynamics of the sub-network composed of hilD, hilC, hilA and downstream-regulators controlling SPI1 genes.

Here we propose a new model focusing on the dynamics of the HilD-HilC-RtsA triangle, since we suppose that its dynamics is the main cause of the expression state of HilA, and therefore of *Salmonella* internalization. First of all, we develope deterministic ODE models; then, we use them as a basis for stochastic models, taking noise – inherently present in biology – into account. Our model is quite general, and we focus on the putative multistability of this subnetwork more than on specific activation or repression parameters, in order to find if the triangle's' topology could be a robust design for its function in pathogenicity. We find indeed that this sub-network could act as a noise-driven switch.

Our predictions are then compared to experimental results from microarray data. These data are in agreement with our model and suggest that it could help to elucidate the mechanisms regulating SPI1 expression.

2 Deterministic models

2.1 Symmetric case

First of all, we consider the hypothesis where all of the three transcription factors, namely HilC, HilD and RtsA, activate their own expression and the expression of each other (see Figure 1 – the repressor HilE is not taken into account at this point –). We will refer to this as the *symmetric case* or S model.

In order to model this system, we take the cue on the mathematical framework proposed by Elowitz and Leibler to derive the equations for the Repressilator system [12]. For each element of the network we consider two variables: the activator protein concentration P and the corresponding mRNA concentration M. Taking into account that, unlike in [12], for the mRNA dynamics we have activation-type relations in the transcription process, we obtain the following set of equations:

$$\begin{aligned} \frac{dM_i}{d\tau} &= -k_M M_i + \sum_{j=1}^{3} \frac{\delta_j K_b P_j^n}{1 + K_b P_j^n} + \delta_0 \\ \frac{dP_i}{d\tau} &= -k_P P_i + k_T M_i, \qquad i = 1, \ldots, 3, \end{aligned} \tag{1}$$

where $i = 1$ corresponds to HilD, $i = 2$ to HilC, and $i = 3$ to RtsA, respectively. Furthermore, here n is the Hill coefficient, k_P is the rate constant for protein degradation, k_M is the rate constant for mRNA degradation, k_T is the rate constant associated with mRNA transcription, δ_i and K_b are rate constants associated with activator binding, and δ_0 models the leakiness of the activators.

Introducing the new variables

$$p_i = \frac{P_i}{K_b^{-1/n}} \qquad m_i = \frac{M_i k_T K_b^{1/n}}{k_P} \qquad t = k_M \tau, \tag{2}$$

system (1) becomes

$$\frac{dm_i}{dt} = -m_i + \sum_{j=1}^{3} \frac{c_j p_j^n}{1+p_j^n} + c \tag{3}$$
$$\frac{dp_i}{dt} = -\beta(p_i - m_i), \qquad i = 1, \ldots, 3,$$

where

$$c_j = \frac{\delta_j k_T K_b^{1/n}}{k_P k_M} \qquad c = \frac{\delta_0 k_T K_b^{1/n}}{k_P k_M} \qquad \beta = \frac{k_P}{k_M}. \tag{4}$$

Therefore, here β denotes the ratio of the protein decay rate to the mRNA decay rate, c_j is the number of protein copies per cell produced from a given promoter type during continuous growth in the presence of saturating amounts of the activator j, and c is the external production term.

Note that both c and the c_j are absolute values and not percentages relative to the global transcription rate, and so they can not be directly compared with experimental results measuring relative transcription rates. To the best of our knowledge, experimental data allowing to estimate accurately the values of these parameters are not available.

We are interested in studying the dynamical behavior of system (3). It is worth observing that, since only positive feedbacks are involved, the system will present only multistability behaviors, and no oscillations can occur [27, 30]. The equilibrium configurations for system (3) are the following:

$$p_i = m_i$$
$$-p_i + \sum_{j=1}^{3} \frac{c_j p_j^n}{1+p_j^n} + c = 0,$$

whereby we deduce that at the steady state we have $\overline{p}_1 = \overline{p}_2 = \overline{p}_3 = p$, with p such that

$$-p + \frac{(c_1+c_2+c_3)p^n}{1+p^n} + c = 0. \tag{5}$$

Since the function $f(p) = \frac{(c_1+c_2+c_3)p^n}{1+p^n} + c$ is monotone increasing, we can conclude that equation (5) can have from one to three solutions, depending on the choice of $\alpha = c_1 + c_2 + c_3$ and c. For $n = 2$ (as in [12]), condition (5) becomes

$$-p + \frac{(c_1+c_2+c_3)p^2}{1+p^2} + c = 0, \tag{6}$$

that is

$$p^3 - (\alpha + c)p^2 + p - c = 0. \tag{7}$$

If we assume the external production c to be zero, then the equilibrium configurations p reduce to be the positive real solutions of equation $-p(1+p^2) + \alpha p^2 = 0$. Thus, we have

$$p = p_c = 0 \qquad \text{and} \qquad p = p_{s,u} = \frac{\alpha \pm \sqrt{\alpha^2 - 4}}{2}.$$

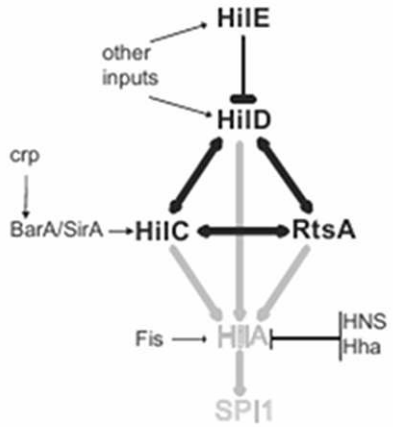

Fig. 1 General model of the signaling network regulating hilA-mediated SPI1 expression.

Therefore, we can conclude that for $\alpha < 2$ we have a unique solution, namely a unique steady state $\overline{p}_1 = \overline{p}_2 = \overline{p}_3 = 0$, where all the three genes are not activated. Instead, for $\alpha > 2$, we have two other solutions, that is two other equilibrium configurations.

As usual, in order to study the stability of the three equilibrium configurations of the global system, we have to consider the associated Jacobian matrix. It is straightforward to see that $m_i = p_i = p_c = 0$ is always stable. Furthermore, in general, the eigenvalues of matrix J are the following:

- $\lambda = -1$ with multiplicity two
- $\lambda = -\beta$ with multiplicity two
- $\lambda_1 = \dfrac{-1-\beta-\sqrt{\beta^2-2\beta+1+4\beta(g'(p_1)+g'(p_2)+g'(p_3))}}{2}$ with multiplicity one
- $\lambda_2 = \dfrac{-1-\beta+\sqrt{\beta^2-2\beta+1+4\beta(g'(p_1)+g'(p_2)+g'(p_3))}}{2}$ with multiplicity one,

where $g'(p_i) = \frac{2c_i p_i}{(1+p_i^2)^2}$.

It is possible to prove that $m_i = p_i = p_u$ is always an unstable equilibrium point, since $\lambda_2|_{m_i=p_i=p_u} > 0$. It is worth observing that for $m_i = p_i = p_u$, the eigenvalue λ_2 has the following expression:

$$\lambda_2 = \frac{-1-\beta+\sqrt{\beta^2-2\beta+1+4\beta\alpha\left(\frac{2p_u}{(1+p_u^2)^2}\right)}}{2};$$

thus, it follows that

$$\lambda_2 > 0 \qquad \text{if and only if} \qquad 2\alpha\frac{p_u}{(1+p_u^2)^2} > 1.$$

Exploiting the algebraic properties of p_u, it yields that this is equivalent to the condition $\alpha p_u < 2$, that is always satisfied for $\alpha > 2$. Thus, we can conclude that the equilibrium configuration $m_i = p_i = p_u$ is always unstable.

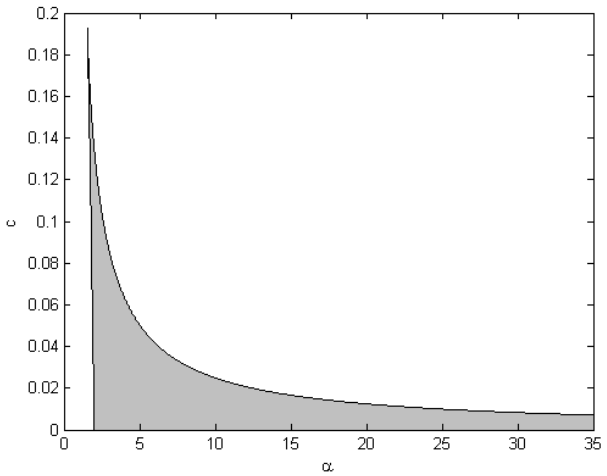

Fig. 2 Boundary of bistable region for the symmetric model in the parameters space $\alpha - c$, defined in (10). The grey region is the bistability one.

On the other hand, we can easily show that $m_i = p_i = p_s$ is asymptotically stable, because $\lambda_2|_{m_i=p_i=p_s} < 0$ holds. In fact, in this case the eigenvalue λ_2 assumes the following form:

$$\lambda_2 = \frac{-1 - \beta + \sqrt{\beta^2 - 2\beta + 1 + 4\beta\alpha\left(\frac{2p_s}{(1+p_s^2)^2}\right)}}{2}.$$

It is easy to observe that

$$\lambda_2 < 0 \qquad \text{if and only if} \qquad 2\alpha\frac{p_s}{(1+p_s^2)^2} < 1.$$

After some algebraic manipulations, it follows that this condition is equivalent to $\alpha p_s > 2$, that is always satisfied for $\alpha > 2$. Thus, we can conclude that the equilibrium configuration $m_i = p_i = p_s$ is stable for all the possible values of $\alpha > 2$.

We are now interested in studying the occurrence of the bistable behavior in the parameters space. In general, it is worth noting that the boundary between the monostability region and the bistability one is precisely defined when equation (7) has two solutions, therefore when a saddle-node bifurcation occurs. A general cubic with two identical roots has the following expression:

$$(p-a)(p-a)(p-\theta a) = p^3 - (2+\theta)ap^2 + (1+2\theta)a^2p - \theta a^3, \tag{8}$$

where θ is the dimensionless ratio of roots. Comparing coefficients of (7) and (8), we find:

$$\begin{aligned} -(\alpha + c) &= -(2+\theta)a \\ 1 &= (1+2\theta)a^2 \\ -c &= -\theta a^3. \end{aligned} \tag{9}$$

Eventually, it is possible to derive the following parametric equations describing the boundary of the bistable region (see Figure 2):

$$\alpha = \frac{2(1+\theta)^2}{\sqrt{(1+2\theta)^3}} \qquad c = \frac{\theta}{\sqrt{(1+2\theta)^3}}. \tag{10}$$

The bistable behavior we derive here mathematically would biologically mean that either this regulatory network is active, with all three proteins present and therefore a cascade activation of HilA and SPI1, or no protein is present among the three, effectively resulting in "non activation" of SPI1 genes. These two states, that could respectively be characterized as pathogenic and non-pathogenic, would indeed form a switch between two completely different lifestyles of *Salmonella*, and the corresponding gene sets.

If such an organization was indeed present, the parameters of the switch, and in particular the environmental conditions allowing to pass from a non-pathogenic to a pathogenic state, would be of great clinical relevance. In the following parts we first check that this bistable dynamics still exist if the system under study is slightly modified.

2.2 Symmetric case with external repressor

In this section we take into account also the repressive action of HilE on HilD (see Figure 1) and study how the behavior of our symmetric system S (3) changes due to this process (SR model). It is worth noting that this case makes more sense with the behavior of the real network, since in nature our three transcription factors are not isolated but are affected by external agents, among which the most important is HilE.

Here, we model the contribution of HilE as an external action, thus without considering the HilE dynamics as an active part of the system. Since HilE binds to HilD, its action mainly reduces the number of free proteins of HilD per cell and then it has been taken into account in the equation for p_1. In particular, the free concentration of p_1 depends on the concentration e of HilE: the more HilE is present, the more HilD is bound, and therefore removed from the system.

Then, our set of equations assumes the following expression:

$$\begin{aligned}
\frac{dm_i}{dt} &= -m_i + \sum_{j=1}^{3} \frac{c_j p_j^n}{1+p_j^n} + c, \qquad i = 1, \dots, 3 \\
\frac{dp_i}{dt} &= -\beta(p_i - m_i), \qquad i \neq 1 \\
\frac{dp_1}{dt} &= -\beta(p_1 - m_1) - \frac{k e p_1}{\theta + e},
\end{aligned} \tag{11}$$

and at equilibrium we have:

$$\begin{aligned}
&\overline{m}_i = \overline{p}_i, \qquad i \neq 1 \\
&\overline{m}_1 = \left(1 + \frac{k}{\beta}\frac{e}{\theta + e}\right)\overline{p}_1 \\
&-\overline{p}_i + \sum_{j=1}^{3} \frac{c_j \overline{p}_j^n}{1 + \overline{p}_j^n} + c = 0 \qquad i \neq 1 \\
&-\left(1 + \frac{k}{\beta}\frac{e}{\theta + e}\right)\overline{p}_1 + \sum_{j=1}^{3} \frac{c_j \overline{p}_j^n}{1 + \overline{p}_j^n} + c = 0.
\end{aligned} \tag{12}$$

It is easy to see that we obtain $\overline{p}_2 = \overline{p}_3$, as in the previous case. Furthermore, we can deduce

$$\sum_{j=1}^{3} \frac{c_j \overline{p}_j^n}{1 + \overline{p}_j^n} + c = \overline{p}_2,$$

that, substituted in the last equation of (12), yields

$$\overline{p}_2 = \left(1 + \frac{k}{\beta}\frac{e}{\theta + e}\right)\overline{p}_1.$$

Finally, we can conclude that the equilibrium configurations for $\overline{p}_1$ are the solutions of the following equation:

$$-\left(1 + \frac{k}{\beta}\frac{e}{\theta + e}\right)\overline{p}_1 + \frac{c_1 \overline{p}_1^n}{1 + p_1^n} + \frac{(c_2 + c_3)\left(1 + \frac{k}{\beta}\frac{e}{\theta + e}\right)^n \overline{p}_1^n}{1 + \left(1 + \frac{k}{\beta}\frac{e}{\theta + e}\right)^n \overline{p}_1^n} + c = 0. \tag{13}$$

For simplicity of notation let us denote $T = \left(1 + \frac{k}{\beta}\frac{e}{\theta + e}\right)$. Furthermore, let us consider $n = 2$ and $c = 0$. Under these assumptions, equation (13) becomes

$$\overline{p}_1 \left(-T + \frac{c_1 \overline{p}_1}{1 + \overline{p}_1^2} + \frac{(c_2 + c_3) T^2 \overline{p}_1}{1 + T^2 \overline{p}_1^2}\right) = 0. \tag{14}$$

Therefore, we have the solution $\overline{p}_1 = 0$, that implies $\overline{p}_2 = \overline{p}_3 = 0$. Moreover, the other steady configurations are the positive real solutions of equation

$$-T^3 p^4 + (c_1 + c_2 + c_3) T^2 p^3 - T(T^2 + 1) p^2 + (c_1 + (c_2 + c_3) T^2) p - T = 0. \tag{15}$$

The trend of these solutions depending on T, for different values of parameters c_1, c_2 and c_3, is shown in Figure 3. It is worth noting that, depending on the choice of the constants c_j, we have different behaviors. In fact, for $c_j = 0.9$ for all j, the system presents a bifurcation: for a critical value T_c of T the two branches of non-zero equilibria collide and disappear. This means that for $T > T_c$ the bistable behavior ceases and there is a unique steady state, where all the three transcription factors are not activated. On the other hand, if we choose $c_j = 1$ for all j, the bistability is preserved for all values of T. Furthermore, the value of these equilibria is decreasing as function of T; this means that the concentrations of p_1 at equilibrium in presence of external repression are lower than in the case when $e = 0$. In Figure 4 the steady state values for the variables p_2 and p_3, as function of T, are represented, as well.

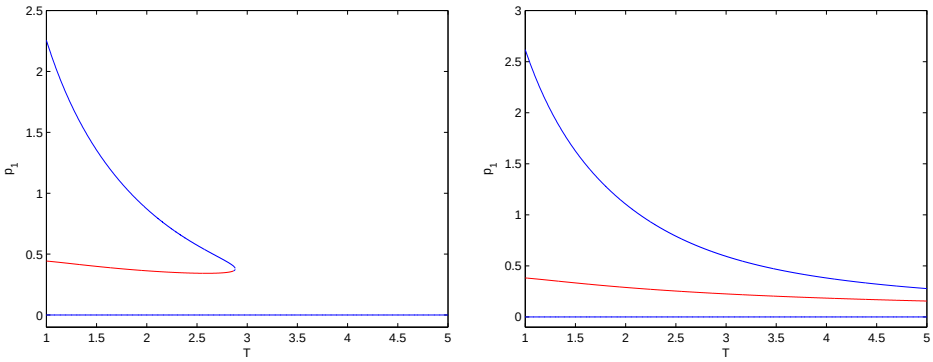

(a) (b)

Fig. 3 Stable (blue) and unstable (red) equilibrium values for the variable p_1, versus the intensity T of the repression action of HilE. Comparison between the case $c_1 = c_2 = c_3 = 0.9$ (a) and the one $c_1 = c_2 = c_3 = 1$ (b).

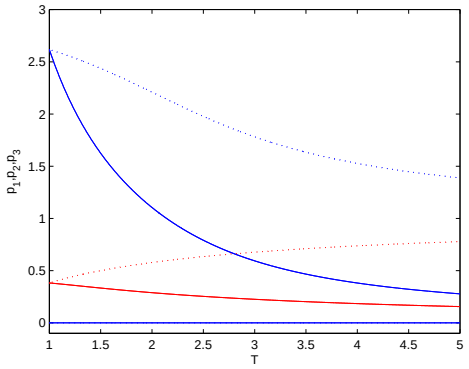

Fig. 4 Stable (blue) and unstable (red) equilibrium configurations in model (11) for the variables p_1(solid line) and $p_2 = p_3$ (dotted line), as function of the repression action T. The chosen parameters are the following: $c_j = 1$ for all $j, c = 0$.

Here we can see an important factor for the external regulation of the triangle switch: depending on the precise dynamical parameters (which actually we do not know about) of the system, the presence of a high concentration of a single repressor could lead to either the loss of the activated pathogenic state, or to a global diminution of the concentration level of all three proteins in the cell. In both cases, this should lead to disactivation – either complete or partial – of the SPI1 regulon, and of the internalization process. Then, a single repressor could turn off the entire operon, a very efficient system. Indeed, it should be noted that, if HilE is the main repressor acting on the system, the CsrA protein has also been shown to repress expression of certain members of the regulatory switch [2], in a way similar to the one of HilE.

In order to characterize the behavior of our system as function of the parameters c_j we exploit the concept of polynomial discriminant. A polynomial discriminant is defined as the product of the squares of the differences of the polynomial roots r_i. For

a polynomial of degree n in the form

$$q(x) = a_n x^n + a_{n-1} x^{n-1} + \cdots + a_1 x + a_0 = 0$$

the discriminant is defined as [8]

$$D_n = a_n^{2n-2} \prod_{\substack{i,j \\ i<j}}^{n} (r_i - r_j)^2. \tag{16}$$

It is worth noting that the discriminant vanishes in presence of a multiple root. Since the boundary of the monostability region and the bistability one for system (11) can be characterized via the appearance of a double real solution in (15), we are interested in finding the relationship that holds among the parameters when the discriminant of (15) is equal to zero.
The discriminant of a quartic equation $q(x) = a_4x^4 + a_3x^3 + a_2x^2 + a_1x + a_0 = 0$ is in general given by

$$\begin{aligned} D_4 = [&(a_1^2\, a_2^2\, a_3^2 \, - 4\, a_1^3\, a_3^3 - 4\, a_1^2\, a_2^3\, a_4 + 18\, a_1^3\, a_2\, a_3\, a_4 \, - 27\, a_1^4\, a_4^2 + 256\, a_0^3\, a_4^3) \\ &+ a_0(-4a_2^3\, a_3^2 \, + 18\, a_1\, a_2\, a_3^3 + 16\, a_2^4\, a_4 - 80\, a_1\, a_2^2\, a_3\, a_4 - 6a_1^2\, a_3^2\, a_4 + 144\, a_1^2\, a_2\, a_4^2) \\ &+ a_0^2(-27\, a_3^4 + 144\, a_2\, a_3^2\, a_4 - 128\, a_2^2\, a_4^2 - 192\, a_1\, a_3\, a_4^2)]. \end{aligned} \tag{17}$$

In our case, for the polynomial in (15), we have

$$a_4 = -T^3 \quad a_3 = (c_1+c_2+c_3)T^2 \quad a_2 = -T(T^2+1) \quad a_1 = c_1+(c_2+c_3)T^2 \quad a_0 = -T.$$

For simplicity of notation, let us denote $B = c_2 + c_3$. Therefore, studying the behavior of the discriminant in the $B - c_1$ parameter space for different values of T we are able to obtain the stability diagram for system (11) (see Figure 5). For $T = 1$, i.e. in absence of repression, we recover the relationship $\alpha = B + c_1 = 2$ for which we have the appearance of a double root in the symmetric model (3) (the solid line in Figure 5). Furthermore, each value of $T = T^* > 1$ identifies a curve in the plane $B - c_1$ that represents the values of B and c_1 such that a transition from bistability to monostability in $T = T^*$ occurs, as in Figure 3(a). For instance, the dashed curve in Figure 5 is plotted for $T^* = 3$. For $T \to \infty$ we get the dotted curve in Figure 5. This means that when $c = 0$ we have essentially three regions of different dynamical behaviors, exhibiting different levels of stability: R_1 is the monostability region for all $T > 1$; in region 2 we have bistability, but at a certain $T = T^*$ this behavior is lost, as in Figure 3(a); in region R_3 we have bistability for all values of T, as in Figure 5).

Actually, when $c > 0$ is considered, we can encounter up to five different behaviors (see Figure 6):

- in region R_1 we have a monostable behavior for every value $T > 1$ of the repressor;
- in region R_2 the system at $T = 1$ is bistable, but there exists a $T = T^* > 1$ such that the bistability disappears and the system becomes monostable;
- in region R_3 the system at $T = 1$ is monostable, but there exists a $T = T^{**} > 1$ such that the system develops a bistability;
- in region R_4 there exist T^* and T^{**} such that the system is bistable for every $T \in [T^{**}, T^*]$;
- in region R_5 the system is bistable for every $T > 1$.

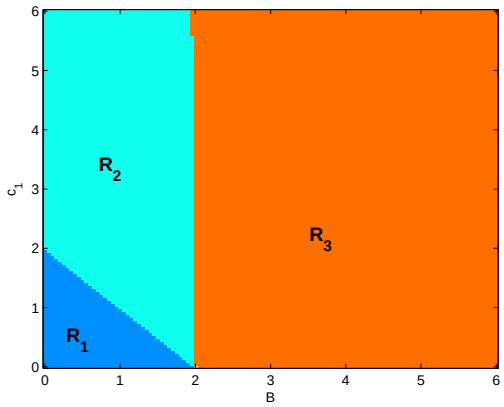

Fig. 5 Stability diagram for system (11). The parameter space is divided in three regions: R_1 is the monostability region for all $T > 1$; in region R_2 (the grey one) we have bistability, but at a certain $T = T^*$ this behavior is lost, as in Figure 3(a); in region R_3 we have bistability for all values of T, as in 3(b).

As it is possible to notice in Figure 6, the greater is the value of $c > 0$ the smaller are the regions R_2, R_3 and R_5. In particular, if we consider a $c > 0.192$ such that the system without repressor is always monostable (see Figure 2), then the system exhibits only regions R_1 and R_4. In particular, the existence of region R_4 in this case is very interesting, because it means that particular values of the repressor can drive the system from a monostable to a bistable regime. Finally, it is possible to show that, if we continue to increase c, we obtain a reduction of region R_4 and at a certain point the system remains monostable for every value of the repressor T.

This last case is biologically quite intuitive: it means that when the basal transcription rate becomes higher and higher, all regulations become inefficient and the genetic system goes into a unique, stable state, driven by the basal transcription. All regimes presented here can find such a putative biological explanation : by example, regimes R_2 and R_3, which seem opposed at first glance, can be explained if one considers that an existing bistability can be dampened in a unique, low state, by an increase in the repressor concentration (regime R_2), while the appearance of bistability with the augmentation of the repressor concentration could occur if the regulatory coefficients c_j are high enough to maintain the system in an high state when repression is low, in which case the repression augmentation would break this single top state and allow for the parallel existence of a low one. Indeed on Figure 6 (a) one can see that the regime R_3 occur at higher c_j values than the regime R_2, corroborating this explanation.

Finally, we can suppose that in standard conditions the basal transcription (i.e. independent of the presence of the others members of the network) is at a low level. Then the multiplicity of the possible regimes depending on the relative values of the c_j parameters and the presence or absence of an external repressor, is a clear indication that very different dynamics, possibly including bistable ones, could be relevant for triggering pathogenicity in *Salmonella*. The tuning of the precise values of these parameters could therefore be the result of a highly complex evolutionary process involving both host-pathogen interactions and pathogen dynamics selection.

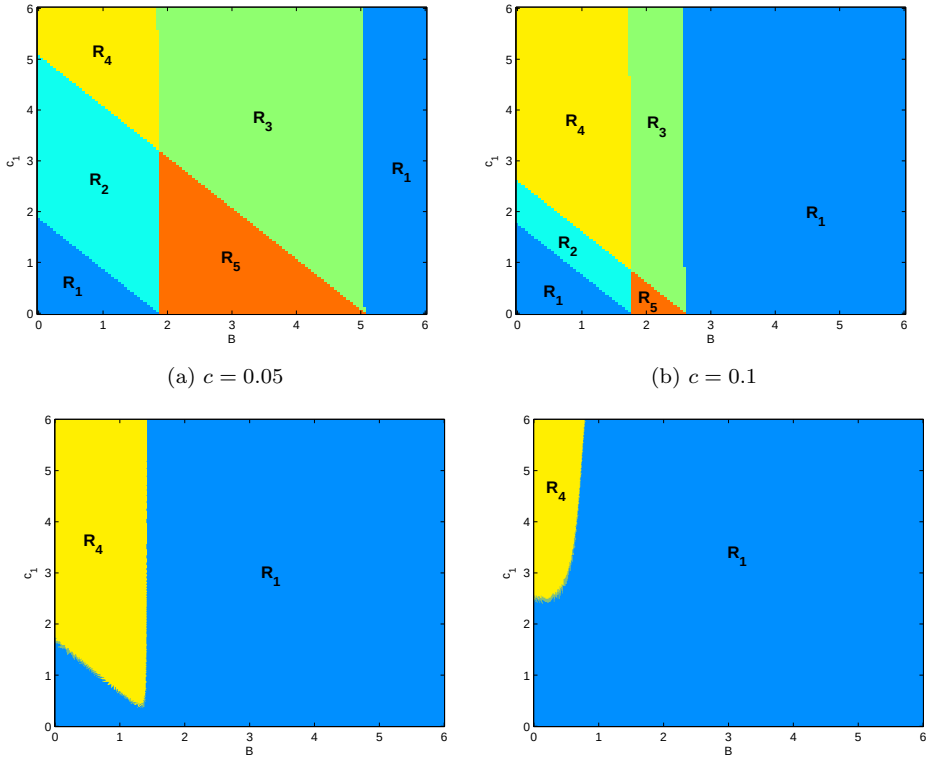

(a) $c = 0.05$ (b) $c = 0.1$

(c) $c = 0.2$ (d) $c = 0.3$

Fig. 6 Stability diagram for system (11) at different values of $c > 0$. The parameter space can be divided in up to five regions: R_1 is the monostability region for all $T > 1$; in region R_2 we have bistability, but at a certain $T = T^*$ this behavior is lost; in region R_3 initially we have monostability, but there exists a $T = T^{**}$ such that the system becomes bistable; in region R_4 there exist $T = T^*$ and $T = T^{**}$ such that the system is bistable only in the interval $[T^{**}, T^*]$. Finally R_5 is the bistability region for all $T > 1$.

2.2.1 Overexpression of HilC

In many experiments directed to study a genetic regulation network, the effects on the global system of overexpressions of specific genes are considered [4, 10]. In our model, an overexpression of a gene i can be suitable represented as a presence of an high external production in the mRNA concentration balance equation for the factor i. Indeed this would model the case where the mRNA is produced from a plasmid and put under control of an artificial promoter, e.g. β-galactose inducible. To model the

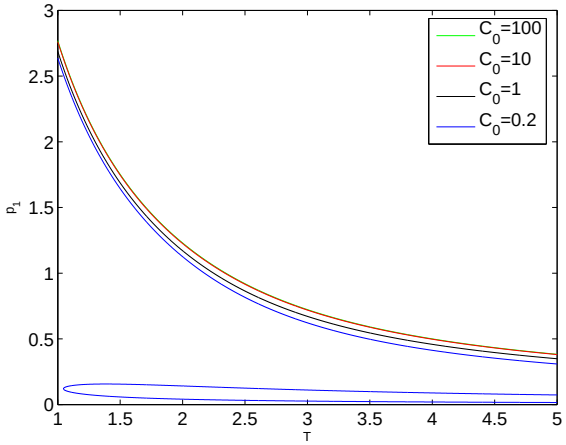

Fig. 7 Equilibrium values for the variable p_1, versus the intensity T of the repression action of HilE, at different values of C_o. The other parameters are chosen as follows: $c_1 = c_2 = c_3 = 1$.

overexpression of the trancriptional activator HilC, equations (11) become (SO model)

$$\begin{aligned}
\frac{dm_i}{dt} &= -m_i + \sum_{j=1}^{3} \frac{c_j p_j^n}{1+p_j^n} + c, \qquad i = 1,3 \\
\frac{dm_2}{dt} &= -m_2 + \sum_{j=1}^{3} \frac{c_j p_j^n}{1+p_j^n} + C_o, \\
\frac{dp_i}{dt} &= -\beta(p_i - m_i), \qquad i \neq 1 \\
\frac{dp_1}{dt} &= -\beta(p_1 - m_1) - \frac{k e p_1}{\theta + e},
\end{aligned} \tag{18}$$

where $c \ll C_o$. It is easy to derive that at equilibrium we have the following relationships:

$$\begin{aligned}
m_2 = p_2 \qquad m_3 = p_3 \qquad m_1 = Tp_1 \\
p_3 = Tp_1 \qquad p_2 = Tp_1 - c + C_o,
\end{aligned}$$

where p_1 is such that

$$-Tp_1 + \frac{c_1 p_1^n}{1+p_1^n} + \frac{c_2 (Tp_1 - c + C_o)^n}{1+(Tp_1 - c + C_o)^n} + \frac{c_3 (Tp_1)^n)}{1+(Tp_1)^n} + c = 0. \tag{19}$$

Thus, for $n = 2$ and $c = 0$ we get

$$-Tp_1 + \frac{c_1 p_1^2}{1+p_1^2} + \frac{c_2 (Tp_1 + C_o)^2}{1+(Tp_1 + C_o)^2} + \frac{c_3 (Tp_1)^2)}{1+(Tp_1)^2} = 0. \tag{20}$$

It is worth observing that Equation (20) can be seen as a fixed point problem $p = f_{C_o}(p)$ where

$$f_{C_o}(p) = \frac{1}{T}\left[\frac{c_1 p^2}{1+p^2} + \frac{c_2 (Tp + C_o)^2}{1+(Tp + C_o)^2} + \frac{c_3 (Tp)^2)}{1+(Tp)^2}\right]. \tag{21}$$

From expression (21) we can derive some characteristics of function f_{C_o}. First of all, it is easy to see that it is monotone increasing as function of the parameter C_o. In fact:

$$\begin{aligned}\frac{\partial f_{C_o}}{\partial C_o} &= \frac{2c_2}{T}\left[\frac{(Tp+C_o)(1+(Tp+C_o))-(Tp+C_o)^2(Tp+C_o)}{(1+(Tp+C_o)^2)^2}\right] \\ &= \frac{2c_2}{T}\frac{(Tp+C_o)}{(1+(Tp+C_o)^2)^2} > 0. \end{aligned} \tag{22}$$

Furthermore, for $C_o \to \infty$, we get

$$\lim_{C_o\to\infty} f_{C_o}(p) = \frac{1}{T}\left[\frac{c_1 p^2}{1+p^2} + c_2 + \frac{c_3(Tp)^2)}{1+(Tp)^2}\right].$$

In Figure 7 the solutions of (20) for different values of C_o are represented. The other parameters have been chosen such that the original SR model (11) without overexpression of HilC displays a bistable behavior, i.e. $c_1 = c_2 = c_3 = 1$. It is interesting to observe that for small values of C_o ($C_o = 0.2$) the bistability is preserved, while increasing the external production rate of HilC we get only one positive real solution, also in absence of HilE ($T = 1$). Furthermore, the equilibrium configuration value for p_1 increases with the increasing of C_o and converges to the solution of the asymptotic equation for $C_o \to \infty$. Therefore the model predicts that a very strong overexpression of HilC – or symmetrically RtsA – should disrupt the bistability of the system, by pushing the entire system in an activated state, either in presence or absence of the repression from HilE.

2.3 Asymmetric case

Some experimental studies [11] show that the activation action of HilD on HilC can be neglected, as this transcriptional activation is much smaller then all others involved in this regulatory system. We are thus interested in studying how our system has to be modified under this assumption (A model). It is straightforward to conclude that in this case the S model (3) becomes

$$\begin{aligned}\frac{dm_i}{dt} &= -m_i + \sum_{j=1}^{3}\frac{c_j p_j^n}{1+p_j^n} + c, \qquad i \neq 2 \\ \frac{dm_2}{dt} &= -m_2 + \frac{c_2 p_2^n}{1+p_2^n} + \frac{c_3 p_3^n}{1+p_3^n} + c \\ \frac{dp_i}{dt} &= -\beta(p_i - m_i), \qquad i = 1,\dots,3. \end{aligned} \tag{23}$$

Let us study how the equilibrium configurations change with respect to those of the symmetric case.

It is easy to derive that at steady state we have the following relations:

$$\begin{aligned}&\overline{m}_i = \overline{p}_i, \qquad i = 1,\dots,3 \\ &\overline{p}_1 = \overline{p}_3 \\ &\overline{p}_2 = \overline{p}_1 - \frac{c_1\overline{p}_1^n}{1+\overline{p}_1^n}, \end{aligned} \tag{24}$$

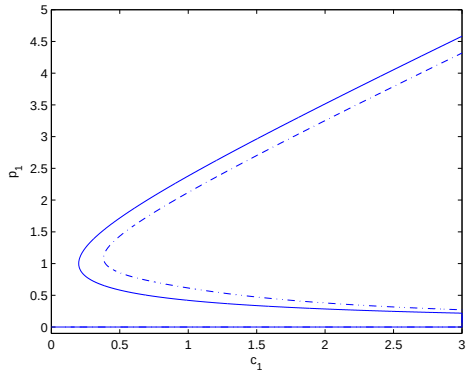

Fig. 8 Equilibrium values for the variable p_1, versus c_1, for $c_2 = c_3 = 0.9$. Comparison between the symmetric model (3) (solid) and the asymmetric one (23) (dashed).

where $\overline{p}_1$ is solution to

$$-\overline{p}_1 + \frac{c_1\overline{p}_1^n}{1+\overline{p}_1^n} + \frac{c_2\left(\overline{p}_1 - \frac{c_1\overline{p}_1^n}{1+\overline{p}_1^n}\right)^n}{1+\left(\overline{p}_1 - \frac{c_1\overline{p}_1^n}{1+\overline{p}_1^n}\right)^n} + \frac{c_3\overline{p}_1^n}{1+\overline{p}_1^n} + c = 0. \tag{25}$$

In the case of Hill coefficient n equal to 2 and in absence of the external production term c, we get

$$-\overline{p}_1 + \frac{c_1\overline{p}_1^2}{1+\overline{p}_1^2} + \frac{c_2\left(\overline{p}_1 - \frac{c_1\overline{p}_1^2}{1+\overline{p}_1^2}\right)^2}{1+\left(\overline{p}_1 - \frac{c_1\overline{p}_1^2}{1+\overline{p}_1^2}\right)^2} + \frac{c_3\overline{p}_1^2}{1+\overline{p}_1^2} = 0. \tag{26}$$

It is possible to see that the solutions of the previous equation are the real positive roots of polynomial

$$\begin{aligned} -p^9 + (3c_1+c_2+c_3)p^8 - (4+3c_1^2+2c_1c_3+2c_1c_2)p^7 \\ + (7c_1+3c_3+c_1^3+c_3c_1^2+3c_2+c_1^2c_2)p^6 \\ - (6+3c_1^2-2c_1c_3-4c_1c_2)p^5 + (5c_1+3c_3+3c_2+c_1^2c_2)p^4 \\ - 2(2+c_1c_2)p^3 + (c_1+c_2+c_3)p^2 - p. \end{aligned} \tag{27}$$

Also in this case, since equation (25) can be viewed as a fixed point problem $\overline{p}_1 = f(\overline{p}_1)$ and f is monotone increasing, we conclude that we can have from one ($\overline{p}_1 = \overline{p}_2 = \overline{p}_3 = 0$) to three solutions, depending on the value of the parameters c_1, c_2 and c_3.

In Figure 8 a comparison between the symmetric model behavior and the asymmetric model one is shown. It is interesting to notice that, for the same choice of c_2 and c_3, the value of c_1 such that the asymmetric system presents a bistable behavior is greater than the one for the symmetric case ($c_1 > 2 - c_2 - c_3$, as we have analytically found above).

If we consider the additional action of the external repressor HilE on the transcription factor HilD, coupling SR and A models, we obtain

$$\begin{aligned}
\frac{dm_i}{dt} &= -m_i + \sum_{j=1}^{3} \frac{c_j p_j^n}{1+p_j^n} + c, \qquad i \neq 3 \\
\frac{dm_2}{dt} &= -m_2 + \frac{c_2 p_2^n}{1+p_2^n} + \frac{c_3 p_3^n}{1+p_3^n} + c \\
\frac{dp_1}{dt} &= -\beta(p_1 - m_1) - \frac{k p_1 e}{\theta + e}, \\
\frac{dp_i}{dt} &= -\beta(p_i - m_i), \qquad i = 2, 3.
\end{aligned} \tag{28}$$

For $n = 2$, $c = 0$ and $T = \left(1 + \frac{k}{\beta}\frac{e}{\theta+e}\right)$, after some algebraic manipulations, we obtain the following equilibrium configurations:

$$\overline{m}_i = \overline{p}_i \ \forall\, i, \qquad \overline{p}_2 = -\frac{c_1 \overline{p}_1^2}{1+\overline{p}_1^2} + T\overline{p}_1 \qquad \text{and} \qquad \overline{p}_3 = T\overline{p}_1,$$

where $\overline{p}_1$ satisfies

$$-T\overline{p}_1 + \frac{c_1 \overline{p}_1^2}{1+\overline{p}_1^2} + \frac{c_2 \left[-\frac{c_1 \overline{p}_1^2}{1+\overline{p}_1^2} + T\overline{p}_1\right]^2}{1+\left[-\frac{c_1 \overline{p}_1^2}{1+\overline{p}_1^2} + T\overline{p}_1\right]^2} + \frac{c_3 T^2 \overline{p}_1^2}{1+T^2\overline{p}_1^2} = 0. \tag{29}$$

It is easy to see that we always have the solution $\overline{p}_1 = 0$, that implies that all the three transcription factors are repressed. In addition, depending on the choice of the parameters c_j, we can have up to three solutions. Therefore, it yields that the asymmetric system can present a bistability behavior as well.

2.4 HilA dynamics

It is well known in literature [10, 11] that HilA is the central regulator in the SPI1 regulation scheme and directly activates the SPI1 genes. Since HilA is activated by the three factors HilD, HilC and RtsA [10, 11], in analogy with the equations written above, the dynamics of HilA can be described by the following nonlinear system:

$$\begin{aligned}
\frac{dm_A}{dt} &= -m_A + \sum_{j=1}^{3} \frac{c_j p_j^n}{1+p_j^n} + c \\
\frac{dp_A}{dt} &= -\beta(p_A - m_A),
\end{aligned} \tag{30}$$

where again $i = 1$ corresponds to HilD, $i = 2$ to HilC, and $i = 3$ to RtsA, respectively.

As equilibrium configuration we get $\overline{m}_A = \overline{p}_A$ and

$$\overline{p}_A = \sum_{j=1}^{3} \frac{c_j \overline{p}_j^n}{1+\overline{p}_j^n} + c.$$

It is worth noting that at equilibrium from the first equation of all the models we have considered - (3),(11), (23) and (28) - it yields

$$-\overline{m}_1 + \sum_{j=1}^{3} \frac{c_j \overline{p}_j^n}{1+\overline{p}_j^n} + c = 0,$$

and therefore we can conclude that $\overline{p}_A = \overline{m}_1$.

In particular, in the cases when the external repressor is not modeled we get $\overline{p}_A = \overline{p}_1$, while when the action of HilE is taken into account we obtain $\overline{p}_A = T\overline{p}_1$, where $T = \left(1 + \frac{k}{\beta}\frac{e}{\theta+e}\right)$ as above. Thus, since p_A is a linear function of p_1, we can conclude that HilA will also exhibit a bistable behavior, depending on the value of the parameters c and c_j.

3 Stochastic models

In the previous section we have modeled our regulatory network via a nonlinear system of ordinary differential equations (ODEs). However, it is well-known that at level of single cells or single genes we mainly encounter noisy processes [23].

There are several ways to suitably describe the noise action in a model for genetic networks [15–17, 19, 29]. In this work we leave out the effects of internal fluctuations (*intrinsic noise*) and we focus on the *external noise* that can be originated by the random variations of control parameters due to the action of agents from the external environment. This type of noise is interesting because it is capable to induce various effects, such as a switch between different configurations [19].

In particular, we exploit a Langevin approach, having supposed that the external noise effect will be small and can be treated as a random perturbation to our existing model. Therefore, our stochastic models will be identical to the deterministic differential equations seen above, except for the addition of a noise term.

The stochastic technique we have considered has been proposed in [18,19], wherein the external noise source enters multiplicatively in order to interact with the degradation rates. Thus, in this case the symmetric model (3) becomes:

$$\begin{aligned} \frac{dm_i}{dt} &= -(1-\gamma\xi_i(t))m_i + \sum_{j=1}^{3} \frac{c_j p_j^n}{1+p_j^n} + c \\ \frac{dp_i}{dt} &= -\beta(1-\gamma\xi_{i+3}(t))p_i + \beta m_i, \qquad i = 1,\dots,3, \end{aligned} \tag{31}$$

where the $\xi_i(t)$ are Gaussian-distributed white noise terms, while the parameter γ serves to increase or decrease the variance. With a simple change of variables

$$m_i = \mathrm{e}^{z_i} \qquad p_i = \mathrm{e}^{w_i} \tag{32}$$

it is possible to easily transform this multiplicative Langevin equation to an additive one. Thus, equation (31) becomes

$$\begin{aligned} \frac{dz_i}{dt} &= -1 + \gamma\xi_i(t) + \frac{1}{\mathrm{e}^{z_i}}\left(\sum_{j=1}^{3} \frac{c_j \mathrm{e}^{nw_j}}{1+\mathrm{e}^{nw_j}} + c\right) \\ \frac{dw_i}{dt} &= -\beta(1-\gamma\xi_{i+3}(t)) + \beta\mathrm{e}^{z_i - w_i}, \qquad i = 1,\dots,3. \end{aligned} \tag{33}$$

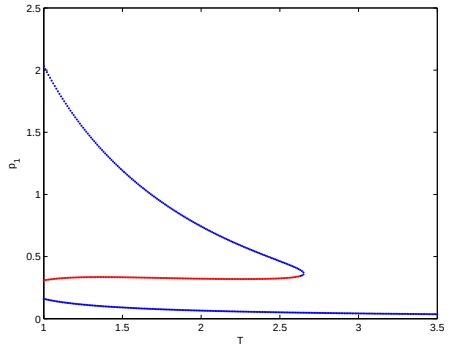

Fig. 9 Stable (blue) and unstable (red) equilibrium configurations of the deterministic model (11) for the variables p_1, as function of the repression action T. We have chosen the parameters as following: $c_j = 0.8$ for all $j, c = 0.1$.

It is worth noting that using this approach we do not have any problem about the positivity of our variables, as we may encounter exploiting different stochastic models [29]. In fact, (32) assures us that we will always obtain $m_i \geq 0$ and $p_i \geq 0$, as it is physically reasonable. Furthermore, the presence of an additive noise term instead of a multiplicative one insures to have a higher order of convergence for the numerical scheme. In fact, in our numerical simulations we exploit the Euler-Maruyama method that has strong order of accuracy equal to 1/2, but it increases to 1 (as the Milstein method) in case of additive noise [22].

However, due to the change of variables (32) we have chosen in order to avoid some pathological problems in the numerical treatment of the system, in the sequel we consider the case $c \neq 0$, where the equilibrium configurations of the deterministic model are strictly greater than zero.

The stochastic version of model (11) where the external repressor HilE is taken into account assumes the following expression:

$$\begin{aligned}
\frac{dz_i}{dt} &= -1 + \gamma\xi_i(t) + \frac{1}{\mathrm{e}^{z_i}}\left(\sum_{j=1}^{3}\frac{c_j \mathrm{e}^{nw_j}}{1+\mathrm{e}^{nw_j}} + c\right) \\
\frac{dw_1}{dt} &= -\beta(T - \gamma\xi_4(t)) + \beta\mathrm{e}^{z_1 - w_1} \\
\frac{dw_i}{dt} &= -\beta(1 - \gamma\xi_{i+3}(t)) + \beta\mathrm{e}^{z_i - w_i}, \qquad i = 2, 3.
\end{aligned} \tag{34}$$

In order to study the effect of external noise on our system, we focus on the following set of parameters $c_1 = c_2 = c_3 = 0.8$, $c = 0.1$. In this case, the deterministic symmetric model presents a bistability in absence of HilE, but this dynamical behavior disappears with increasing repressor action T (see Figure 9). We show that, depending on the values of the repressor action T and noise intensity γ, the stochastic system can have different behaviors. In particular, it is possible to see that, although the deterministic system presents monostability for certain values of these parameters, the stochastic system can exhibit switching between two configurations.

First of all, let us consider the case of absence of HilE, that is $T = 1$. The deterministic system $\gamma = 0$ presents two stable configurations: $\overline{p}_{1A} = \overline{m}_{1A} = \overline{p}_{2A} = \overline{p}_{3A} =$

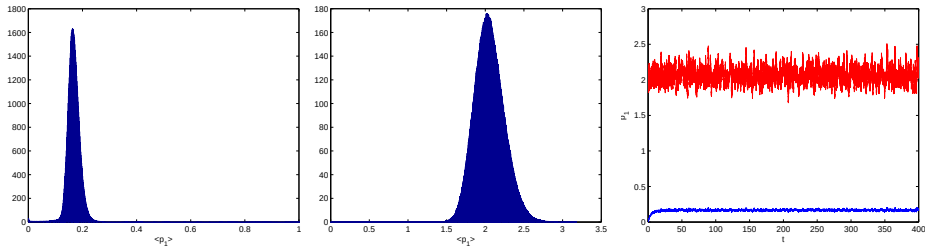

(a) (b) (c)

Fig. 10 Stochastic system with $T = 1$ and $\gamma = 0.1$. Histograms over 100 realizations with initial conditions around the lower (a) and the higher (b) equilibria of the deterministic model (only the variable p_1 is here displayed). In (c) two simulations of system (34) are represented. In absence of repressor and low values of noise we do not have transitions between the two configurations.

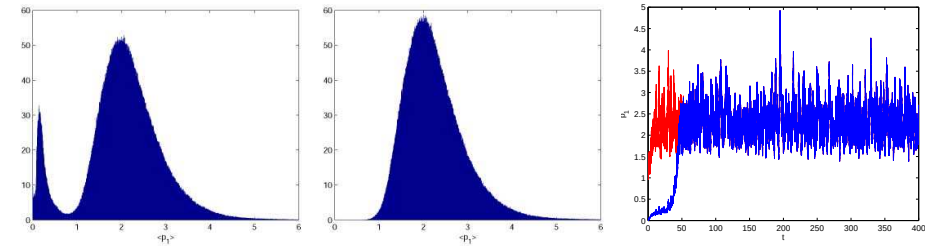

(a) (b) (c)

Fig. 11 Stochastic system with $T = 1$ and $\gamma = 0.3$. Histograms over 100 realizations with initial conditions around the lower (a) and the higher (b) equilibria of the deterministic model (only the variable p_1 is here displayed). In (c) two simulations of system (34) are represented. As it is possible to see, we can have transitions from the lower to the higher configuration, but not the opposite.

$\overline{m}_{2A} = \overline{m}_{3A} = 0.1596$ and $\overline{p}_{1B} = \overline{m}_{1B} = \overline{p}_{2B} = \overline{p}_{3B} = \overline{m}_{2B} = \overline{m}_{3B} = 2.0322$. For small values of the noise ($\gamma = 0.1$), if the system starts close to the two equilibria, it remains in the same basin of attraction since the two stable configurations are too far from each other (see Figure 10). With a higher noise intensity ($\gamma = 0.3$), the trajectories that start from the lower equilibrium are able to cross the separatrix and fluctuate around the higher configuration, but they cannot go back to the initial attractor, since the noise is not sufficient (see Figure 11). Thus, in this case, we can have transitions from A to B but not the opposite.

On the other hand, Figure 12 shows that for $T = 2.5$ and $\gamma = 0.1$ we can have transitions from the higher equilibrium ($\overline{p}_{1B} = \overline{m}_{1B} = 0.462$, $\overline{p}_{2B} = \overline{p}_{3B} = \overline{m}_{2B} = \overline{m}_{3B} = T\overline{p}_{1B} = 1.155$) to the lower one ($\overline{p}_{1A} = \overline{m}_{1A} = 0.0511$, $\overline{p}_{2A} = \overline{p}_{3A} = \overline{m}_{2A} = \overline{m}_{3A} = T\overline{p}_{1A} = 0.1277$), but not the opposite. This is due to the fact that the separatrix is closer to the configuration B and the noise is not sufficient to drive the system from A to B. Increasing the noise intensity up to $\gamma = 0.5$ we become to have jumps between the two configurations, as in Figure 13.

The most interesting phenomenon arises for $T > 2.652$ and involves the appearance of a bistable behavior due to the noise where the deterministic model shows monostability. (see Figure 14). In fact for such choice of T the deterministic model (11) presents a single equilibrium point ($\overline{p}_1 = \overline{m}_1 = 0.0422$, $\overline{p}_2 = \overline{p}_3 = \overline{m}_2 = \overline{m}_3 = T\overline{p}_1 = 0.1266$).

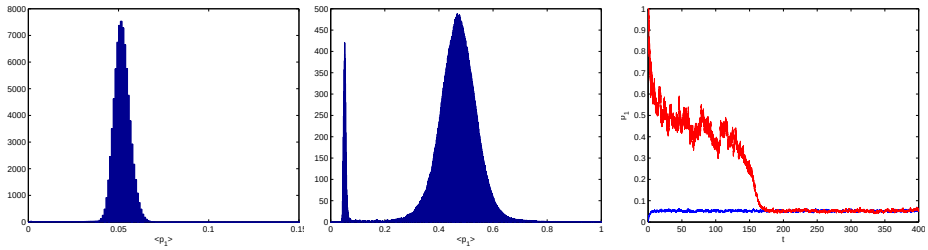

(a) (b) (c)

Fig. 12 Stochastic system with $T = 2.5$ and $\gamma = 0.1$. Histograms over 100 realizations with initial conditions around the lower (a) and the higher (b) equilibria of the deterministic model (only the variable p_1 is here displayed). In (c) two simulations of system (34) are represented. As it is possible to see, we can have transitions from the higher to the lower configuration, but not the opposite.

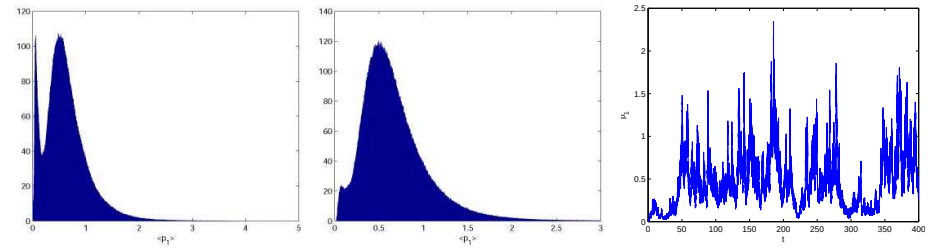

(a) (b) (c)

Fig. 13 Stochastic system with $T = 2.5$ and $\gamma = 0.5$. Histograms over 100 realizations with initial conditions around the lower (a) and the higher (b) equilibria of the deterministic model (only the variable p_1 is here displayed). In (c) a simulation of system (34) is represented. As it is possible to see, we can have jumps between the two configurations.

However, for initial conditions close to this steady state, the stochastic model may not converge to the unique configuration where all the factors are not activated but new dynamics take place. In Figure 14 it is possible to observe that the noise fluctuations can induce a switch process between the deterministic steady state and a new higher value of concentration, giving rise to a bistable behavior.

Biologically, this would mean that *Salmonella* could use fluctuations in its environment, or internal molecular noise, to switch between a non-pathogenic and a pathogenic state, allowing for a large panel of noise dependent controls of SPI1 activation and pathogenicity.

Our model then predicts two main features for the regulation of HilA and SPI1, bistability and noise dependence. We now use available experimental data to show that these features are indeed observed *in vivo*.

4 Comparison with large-scale experimental data

Experimental data concerning the precise dynamics of the three genes HilD, HilC and RtsA are still scarcely available, therefore making very hard to infer the parameters involved, e.g. transcriptional activation coefficients, even if this has been tried [14]. Here we use microarray expression data in order to show how they reflect certain

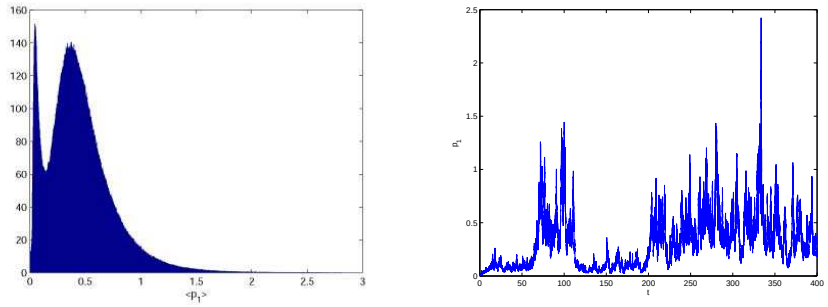

(a) (c)

Fig. 14 Stochastic system with $T = 2.5$ and $\gamma = 0.5$. Histograms over 100 realizations with initial conditions around the unique equilibrium of the deterministic model (only the variable p_1 is here displayed). In (b) the evolution of p_1 obtained by simulation of equation (34) is represented. In this case we have the emergence of a new configuration with a higher value of concentration.

characteristics of our model, in particular bistability. Given the relatively small size of our dataset, we must emphasize that these results can not be considered as a very strong evidence in favor of the hypothesis of bistability in the living cells of *Salmonella*, but nevertheless provide an experimental indication showing that bistability could occur in this system.

We downloaded all available data (57 microarrays) for the expression of genes HilA, HilD, HilC, RtsA and HilE, in *S. enterica* serovar Typhimurium from the Stanford Microarray Database [6,7,9,24]. In order to check our hypothesis, we compared the values of expression in different environmental conditions and computed the correlation coefficients between these five genes on the entire dataset. These correlation coefficients (see Table 1) were high (and significantly different from 0, $p < 2.10^{-13}$ for each correlation) between all genes excepted HilE, with whom no correlation – either positive or negative – could be seen. The high correlation between these genes corroborates our model, in which mRNA levels of these genes should be equal (symmetric case) or linearly related (*SR* model). Note that as the interaction between HilE and HilD is a protein-protein interaction, their expression levels as measured by the microarray can not be used neither to confirm or infirm our model.

HilA	HilC	HilD	RtsA	HilE
HilA	0.928	0.910	0.874	0.141
HilC		0.823	0.792	0.203
HilD			0.841	0.077
RtsA				0.112

Table 1 Pearson correlation coefficient between HilA, HilC, HilD, RtsA and HilE, computed on 57 microarrays.

To show the presence of a bistable behavior in this microarray dataset, we used a clustering approach. Namely, we computed the average of the expression levels of HilD, HilC and RtsA in each dataset, and clustered the 57 obtained values using a Gaussian mixture model with unequal variance. The BIC criterion was used to discriminate

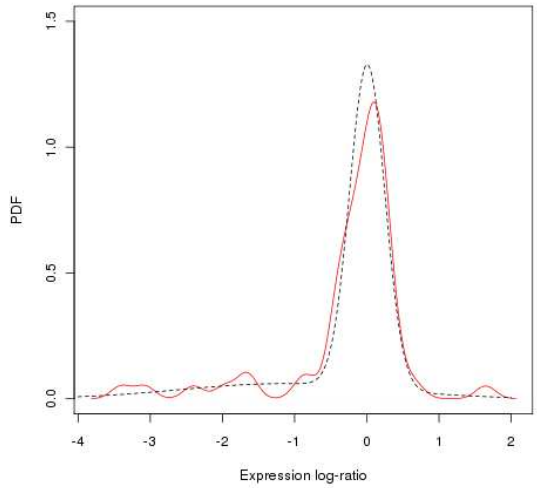

Fig. 15 Distribution of the average of HilC-HilD-RtsA expression values. Black dashed lines, real data; black solid lines, the two-cluster model with a low expression "off" state and a regular expression "on" state.

between group numbers [26]. Computations were done using the R Mclust package [13] with default parameters.

Results of this analysis are presented in Figure 15. The best model is a two cluster model, with one highly populated cluster (48 out of 57 points) representing the activated state, and 9 points in the off state, where all expression ratios are very low. The fact that points with a standard expression value do correspond to the "on" state is not surprising, as experimentally *Salmonella* laboratory cells tend to naturally express the SPI-1 operon in standard culture condition, even without contact with human cells.

5 Conclusion

In this work, we show that the regulatory triangle of the SPI1 could act as a noise-driven switch, by controlling the expression of the transcriptional regulator HilA, which in turn activates the internalization operon. Our model is flexible and can account for either a completely symmetric regulation or an asymmetric one, and incorporate the effect of an external regulation on the system, such as the repression of HilD by HilE, which has been experimentally shown. Moreover our model is in good agreement with the experimental expression data from microarrays.

The regulatory sub-network presents bistable dynamics, where the two different states could be thought of as a pathogenic and a non-pathogenic state. Such an organization would make good biological sense, and allow for a clear decoupling of the genetic resources used during infection or not. Obviously, this central core of regulators (HilC, HilD, RtsA, HilE) would integrate multiple signaling inputs, as many sensors have been described and shown to regulate the activation of pathogenicity; but a noise-driven switch would nevertheless be a simple way of regulation, including complex sensors for population density or physiological state of the host. A bistable

system thereby is very well suited for such an integration task, as a stochastic component avoids "all or none" type of responses, and allows for greater robustness of the population of infecting Salmonella. Furthermore, rather than hard-wiring genetically transcriptional responses to a possibly great variety of environmental clues and combinations thereof, a switch driven by external noise (possibly accumulating over different inputs) promises greatest flexibility at lowest cost.

In order to experimentally test our model one would need to modify the sensitivity of the regulatory switch to noise in strains of *Salmonella*, and then observe the pathogenicity of the engineered strains. Such experiments require a deep knowledge of the parameters governing the dynamics of the system, which we still cannot compute. Dedicated experiments could provide good approximations of those, and also provide means to test the system under conditions where these parameters have been artificially influenced. Indeed, a good knowledge of the SPI1 switch could allow the design of a molecule that would prevent the switch to the "on" state, thereby preventing pathogenicity from *Salmonella* without making use of antibiotics.

Author contributions

VL developed the model and made all theoretical and numerical computations. MBB analyzed experimental data. All authors designed the project and wrote the paper.

References

1. Ackermann, M., Stecher, B., Freed, N.E., Songhet, P., Hardt, W.D., Doebeli, M.: Self-destructive cooperation mediated by phenotypic noise. Nature **454**(7207), 987–990 (2008). DOI 10.1038/nature07067. URL http://dx.doi.org/10.1038/nature07067
2. Altier, C.: Genetic and environmental control of salmonella invasion. J Microbiol **43 Spec No**, 85–92 (2005)
3. Bajaj, V., Hwang, C., Lee, C.A.: hila is a novel ompr/toxr family member that activates the expression of salmonella typhimurium invasion genes. Mol Microbiol **18**(4), 715–727 (1995)
4. Baxter, M.A., Fahlen, T.F., Wilson, R.L., Jones, B.D.: Hile interacts with hild and negatively regulates hila transcription and expression of the salmonella enterica serovar typhimurium invasive phenotype. Infect Immun **71**(3), 1295–1305 (2003)
5. Bustamante, V.H., Martnez, L.C., Santana, F.J., Knodler, L.A., Steele-Mortimer, O., Puente, J.L.: Hild-mediated transcriptional cross-talk between spi-1 and spi-2. Proc Natl Acad Sci U S A **105**(38), 14,591–14,596 (2008). DOI 10.1073/pnas.0801205105. URL http://dx.doi.org/10.1073/pnas.0801205105
6. Chan, K., Baker, S., Kim, C.C., Detweiler, C.S., Dougan, G., Falkow, S.: Genomic comparison of salmonella enterica serovars and salmonella bongori by use of an s. enterica serovar typhimurium dna microarray. J Bacteriol **185**(2), 553–563 (2003)
7. Chan, K., Kim, C.C., Falkow, S.: Microarray-based detection of salmonella enterica serovar typhimurium transposon mutants that cannot survive in macrophages and mice. Infect Immun **73**(9), 5438–5449 (2005). DOI 10.1128/IAI.73.9.5438-5449.2005. URL http://dx.doi.org/10.1128/IAI.73.9.5438-5449.2005
8. Cohen, H.: A Course in Computational Algebraic Number Theory. Springer New York (1993)
9. Detweiler, C.S., Monack, D.M., Brodsky, I.E., Mathew, H., Falkow, S.: virk, soma and rcsc are important for systemic salmonella enterica serovar typhimurium infection and cationic peptide resistance. Mol Microbiol **48**(2), 385–400 (2003)
10. Ellermeier, C., Ellermeier, J., Slauch, J.: HilD, HilC and RtsA constitute a feed forward loop that controls expression of the SPI1 type three secretion system regulator hilA in Salmonella enterica serovar Typhimurium. Molecular Microbiology **57**(3), 691–705 (2005)

11. Ellermeier, J., Slauch, J.: Adaptation to the host environment: regulation of the SPI1 type III secretion system in Salmonella enterica serovar Typhimurium. Current Opinion in Microbiology **10**(1), 24–29 (2007)
12. Elowitz, M., Leibler, S.: A synthetic oscillatory network of transcriptional regulators. Nature **403**(6767), 335–338 (2000)
13. Fraley, C., Raftery, A.E.: Model-based clustering, discriminant analysis, and density estimation. Journal of the American Statistical Association **97**, 611–631 (2002)
14. Ganesh, A.B., Rajasingh, H., Mande, S.S.: Mathematical modeling of regulation of type iii secretion system in salmonella enterica serovar typhimurium by sira. In Silico Biol **9**(1-2), S57–S72 (2009)
15. Gardiner, C.: Handbook of Stochastic Methods. Springer New York (1983)
16. Gillespie, D.: Exact stochastic simulation of coupled chemical reactions. The Journal of Physical Chemistry **81**(25), 2340–2361 (1977)
17. Gillespie, D.: The chemical Langevin equation. The Journal of Chemical Physics **113**(1), 297–306 (2000)
18. Hasty, J., Isaacs, F., Dolnik, M., McMillen, D., Collins, J.: Designer gene networks: Towards fundamental cellular control. Chaos: An Interdisciplinary Journal of Nonlinear Science **11**, 207–220 (2001)
19. Hasty, J., Pradines, J., Dolnik, M., Collins, J.: Noise-based switches and amplifiers for gene expression. Proceedings of the National Academy of Sciences **97**(5), 2075–2080 (2000)
20. Hautefort, I., Proena, M.J., Hinton, J.C.D.: Single-copy green fluorescent protein gene fusions allow accurate measurement of salmonella gene expression in vitro and during infection of mammalian cells. Appl Environ Microbiol **69**(12), 7480–7491 (2003)
21. Jones, B.D.: Salmonella invasion gene regulation: a story of environmental awareness. J Microbiol **43 Spec No**, 110–117 (2005)
22. Kloeden, P., Platen, E.: Numerical Solution of Stochastic Differential Equations. Springer, Berlin (1992)
23. Maheshri, N., O'Shea, E.: Living with noisy genes: how cells function reliably with inherent variability in gene expression. Annu. Rev. Biophys. Biomol. Struct. **36**, 413–434 (2007)
24. Prouty, A.M., Brodsky, I.E., Falkow, S., Gunn, J.S.: Bile-salt-mediated induction of antimicrobial and bile resistance in salmonella typhimurium. Microbiology **150**(Pt 4), 775–783 (2004)
25. Schlumberger, M.C., Mller, A.J., Ehrbar, K., Winnen, B., Duss, I., Stecher, B., Hardt, W.D.: Real-time imaging of type iii secretion: Salmonella sipa injection into host cells. Proc Natl Acad Sci U S A **102**(35), 12,548–12,553 (2005). DOI 10.1073/pnas.0503407102. URL http://dx.doi.org/10.1073/pnas.0503407102
26. Schwarz, G.E.: Estimating the dimension of a model. Annals of Statistics **6(2)**, 461–464 (1978)
27. Sontag, E.: Molecular systems biology and control. European Journal of Control **11**(5), 396–435 (2005)
28. Temme, K., Salis, H., Tullman-Ercek, D., Levskaya, A., Hong, S.H., Voigt, C.A.: Induction and relaxation dynamics of the regulatory network controlling the type iii secretion system encoded within salmonella pathogenicity island 1. J Mol Biol **377**(1), 47–61 (2008). DOI 10.1016/j.jmb.2007.12.044. URL http://dx.doi.org/10.1016/j.jmb.2007.12.044
29. Toulouse, T., Ao, P., Shmulevich, I., Kauffman, S.: Noise in a small genetic circuit that undergoes bifurcation. Complexity **11**(1), 45–51 (2005)
30. Tyson, J., Othmer, H.: The dynamics of feedback control circuits in biochemical pathways. Progress in Theoretical Biology **5**, 1–62 (1978)